Spin Polarization Simulations for the Future Circular Collider e+e- using BMAD

Yi Wu[1], Félix Carlier[2], Tatiana Pieloni[1]

[1]École Polytechnique Fédérale de Lausanne (EPFL)
[2]The European Organization for Nuclear Research (CERN)

Acknowledgments to Alain Blondel, Desmond Barber, David Sagan, Eliana Gianfelice-Wendt, Tessa Charles, Werner Herr, Léon Van Riesen-Haupt and all colleagues

EPFL CERN CHART Swiss Accelerator Research and Technology

Outline

Motivation

- FCC-ee, the first step of the FCC project, will offer high precision explorations of physics at four center-of-mass energies.
- The high precision center-of-mass energy calibration is feasible at Z and W energies by means of resonant depolarization.
- Spin simulations for the validation of the energy calibration method
- Effects of lattice perturbations on spin polarization should be investigated.
- Sufficient polarization levels under various possible lattice conditions
- BMAD, a simulation tool that allows full lattice control and the spin simulations

BMAD Home Page, https://www.classe.cornell.edu/bmad/

Spin Precession and Descriptions

Thomas-BMT equation that describes spin precessions under electromagnetic field

$$\frac{\mathrm{d}\hat{S}}{\mathrm{d}s} = \left(\vec{\Omega}^{c.o}(s) + \vec{\omega}^{s.b}(\vec{u};s)\right) \times \hat{S}$$
$$\vec{u} \equiv (x, x', y, y', z, \delta)$$

Spin rotation matrix for closed orbit solution

$$\hat{S}(s) = \mathbf{R}_{c.o}(s, s_i)\hat{S}(s_i)$$

$\hat{n}_0(s) \Rightarrow$ Periodic and stable spin direction on the closed orbit

$\nu_0 \Rightarrow$ Number of spin processions around $\hat{n}_0$ per turn on the closed orbit / closed orbit spin tune

$\nu_0 = a\gamma$ in the perfectly aligned flat ring without solenoids

Invariant Spin Field

EPFL

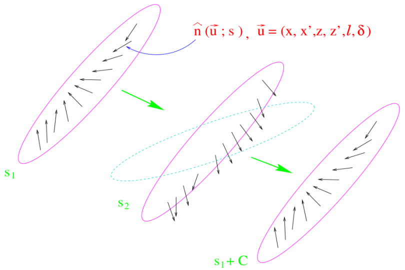

Figure: The variation of the invariant spin field $\hat{n}(\vec{u}; s)$ within the same phase space region (encircled by the solid line) at three azimuths.

$\hat{n}(\vec{u}; s)$

- invariant spin *field*
- the one-turn periodic unit vector that satisfies the T-BMT equation depending on $(\vec{u}; s)$
- the direction of the equilibrium polarization at $(\vec{u}; s)$
- $\hat{n}(\vec{u}; s)=\hat{n}(\vec{u}; s + C)$
- $\hat{n}(\vec{M}(\vec{u}; s); s + C) = \mathbf{R}(\vec{u}; s)\hat{n}(\vec{u}; s)$
- $\hat{n}(\vec{u}; s)$ reduces to $\hat{n}_0(s)$ on the closed orbit

Figure from M. Berglund, Spin-orbit maps and electron spin dynamics for the luminosity upgrade project at HERA

Polarization Build-Up

EPFL

- Sokolov-Ternov (ST) effect: spin-flip synchrotron radiation emission

$$P_{ST} = \frac{W_{\uparrow\downarrow} - W_{\downarrow\uparrow}}{W_{\uparrow\downarrow} + W_{\downarrow\uparrow}} \simeq 92.38\% \quad \text{and} \quad \tau_{ST}^{-1} = \frac{5\sqrt{3}}{8}\frac{r_e\gamma^5\hbar}{m_e|\rho|^3}$$

- Baier-Katkov-Strakhovenko (BKS) polarization level

$$\vec{P}_{BKS} = -\frac{8}{5\sqrt{3}}\hat{n}_0 \frac{\oint \mathrm{d}s \frac{\hat{n}_0(s)\cdot\hat{b}(s)}{|\rho(s)|^3}}{\oint \mathrm{d}s \frac{\left[1-\frac{2}{9}(\hat{n}_0\cdot\hat{s})^2\right]}{|\rho(s)|^3}}$$

$$\tau_{BKS}^{-1} = \frac{5\sqrt{3}}{8}\frac{r_e\gamma^5\hbar}{m_e}\frac{1}{C}\oint \mathrm{d}s \frac{\left[1-\frac{2}{9}\left(\hat{n}_0\cdot\hat{s}\right)^2\right]}{|\rho(s)|^3}$$

Spin Diffusion

EPFL

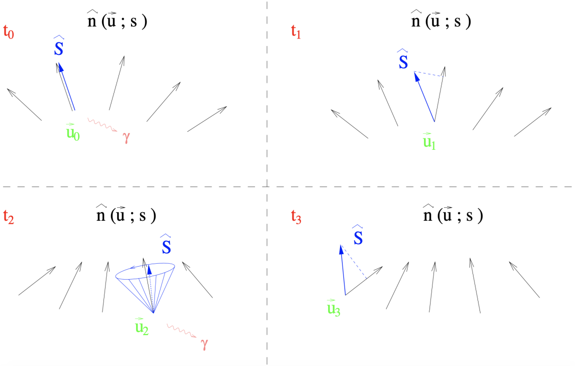

Figure: A simple illustration of the spin diffusion after two photon emissions

- For a single electron, a large number of stochastic photon emissions result in a random walk of $|\hat{S} \cdot \hat{n}|$.
- The total polarization level of a beam is decreased.

Figure from M. Berglund, Spin-orbit maps and electron spin dynamics for the luminosity upgrade project at HERA

Polarization Build-Up with Radiative Depolarization

EPFL

- ST effect + radiative depolarization → equilibrium polarization
- Derbenev–Kondratenko–Mane (DKM) formula when radiative depolarization is considered

$$P_{DK} = -\frac{8}{5\sqrt{3}} \times \frac{\oint \mathrm{d}s \left\langle \frac{1}{|\rho(s)|^3} \hat{b} \cdot \left(\hat{n} - \frac{\partial \hat{n}}{\partial \delta} \right) \right\rangle_s}{\oint \mathrm{d}s \left\langle \frac{1}{|\rho(s)|^3} \left(1 - \frac{2}{9} \left(\hat{n} \cdot \hat{s} \right)^2 + \frac{11}{18} \left(\frac{\partial \hat{n}}{\partial \delta} \right)^2 \right) \right\rangle_s}$$

$$\tau_{DK}^{-1} = \tau_{BKS}^{-1} + \tau_{dep}^{-1}$$

$$\tau_{dep}^{-1} = \frac{5\sqrt{3}}{8} \frac{r_e \gamma^5 \hbar}{m_e} \frac{1}{C} \oint \mathrm{d}s \left\langle \frac{\frac{11}{18} \left(\frac{\partial \hat{n}}{\partial \delta} \right)^2}{|\rho(s)|^3} \right\rangle_s$$

- $\partial \hat{n} / \partial \delta$: the spin-orbit coupling function

Spin Resonances

Integer resonance $\nu_0 = m$

- the small perturbations have an overwhelming impact
- $\hat{n}_0(s)$ deviates from vertical direction
- loss of polarization accumulation

Spin-orbit resonances $\nu_0 = m + m_x Q_x + m_y Q_y + m_z Q_z$

- $|m_x| + |m_y| + |m_z| = 1$ first order spin-orbit resonances
- Away from resonance $\Rightarrow \hat{n}(\vec{u}; s)$ almost aligned with $\hat{n}_0(s)$
- Near resonances $\Rightarrow \hat{n}(\vec{u}; s)$ deviates from $\hat{n}_0(s) \Rightarrow$ large $\partial\hat{n}/\partial\delta \Rightarrow$ lower polarization

Linear Polarization Calculation

SLIM formalism for linearized orbital and spin motions

- 6×6 orbital transfer matrix $\rightarrow$ 8×8 spin-orbit transfer matrix

$$\mathbf{T}_{8\times 8} = \begin{pmatrix} \mathbf{M}_{6\times 6} & \mathbf{0}_{6\times 2} \\ \mathbf{G}_{2\times 6} & \mathbf{D}_{2\times 2} \end{pmatrix}$$

- spin-orbit vector $(x, x', y, y', z, \delta, \alpha, \beta)$ with respect to the closed orbit
- $\vec{S} \approx \hat{n}_0 + \alpha \hat{m} + \beta \hat{l}$, unit along $\hat{n}_0$, small deviation from $\hat{n}_0$

$$P_{DK} = -\frac{8}{5\sqrt{3}} \times \frac{\oint \mathrm{d}s \left\langle \frac{1}{|\rho(s)|^3} \hat{b} \cdot \left(\hat{n} - \frac{\partial \hat{n}}{\partial \delta}\right) \right\rangle_s}{\oint \mathrm{d}s \left\langle \frac{1}{|\rho(s)|^3} \left(1 - \frac{2}{9} \left(\hat{n} \cdot \hat{s}\right)^2 + \frac{11}{18} \left(\frac{\partial \hat{n}}{\partial \delta}\right)^2\right) \right\rangle_s}$$

- $\langle \hat{n} \rangle_s \rightarrow \hat{n}_0(s)$
- neglect $\hat{b} \cdot \partial \hat{n} / \partial \delta$
- $\partial \hat{n} / \partial \delta$, ignores its dependence on the phase space position

Tao (BMAD)

SLIM formalism from A.W. Chao, Evaluation of radiative spin polarization in an electron storage ring

Nonlinear Spin Tracking Simulations

EPFL

- Avoid the introduction of $\hat{n}$
- Independent of spin diffusion theory
- Obtain τ_{dep} via Monte-Carlo spin tracking simulations
- P_{BKS} and τ_{BKS} are computed at closed orbit

$$P(t) = P_{DK}\left[1 - e^{-t/\tau_{DK}}\right] + P_0 e^{-t/\tau_{DK}} \simeq P_0 e^{-t/\tau_{dep}}$$

$$P_{eq} \simeq P_{BKS}\frac{\tau_{dep}}{\tau_{BKS} + \tau_{dep}}$$

Long-Term Tracking

Main Lattice Parameters

EPFL

Sequence 217 at Z energy is used in the simulations

Circumference (km)	97.756
Beam energy (GeV)	45.6
β_x^* (m)	0.15
β_y^* (mm)	0.8
ϵ_x (nm)	0.27
ϵ_y (pm)	1
Synchrotron tune Q_z	0.025
Horizontal tune Q_x	269.139
Vertical tune Q_y	269.219

Table: Main parameters at Z energy

FCC collaboration. (2019). FCC-ee: The Lepton Collider: Future Circular Collider Conceptual Design Report Volume 2. European Physical Journal: Special Topics, 228(2), 261-623.

Effective Model

EPFL

- Use an effective model to simulate realistic orbits after lattice correction
- The errors are randomly distributed obeying the truncated Gaussian distributions (truncated at $2.5\,\sigma$)

Residual errors after lattice correction

Type	$\sigma_{\Delta \mathrm{X}}$ (μm)	$\sigma_{\Delta \mathrm{Y}}$ (μm)	$\sigma_{\Delta \mathrm{S}}$ (μm)	$\sigma_{\Delta \mathrm{PSI}}$ (μrad)	$\sigma_{\Delta \mathrm{THETA}}$ (μrad)	$\sigma_{\Delta \mathrm{PHI}}$ (μrad)
Arc quadrupole	0.1	0.1	0.1	2	2	2
Arc sextupole	0.1	0.1	0.1	2	2	2
Dipoles	0.1	0.1	0.1	2	0	0
IR quadrupole	0.1	0.1	0.1	2	2	2
IR sextupole	0.1	0.1	0.1	2	2	2

Table: An effective model for the small error generation used in the spin-orbit simulations

Preliminary Global Parameters Matching in BMAD

EPFL

- Match the global parameters with the designed values
- Simplified matching: using the elements in RF section
- Optimized matching: adding BPMs, kickers and correctors

	Step order	"Data"	"Variables"
No err	1	x and z at IPs, Q_z	phi0, voltage
	2	β^*, Q_x, Q_y	correctors, RF Quad
	3	(recheck Data in step 1)	(phi0, voltage)
	4	save orbits at BPMs	
Add err	5	orbits at BPMs and IPs (higher weight)	kickers
	6	β^*, Q_x, Q_y	correctors, RF quad
	7	x and z at IPs, Q_z	phi0, voltage

Table: The optimized procedures for the parameter matching

Future orbit corrections and parameter matching will be done in MADX

Energy Scan in Tao (BMAD)

- Tao computes the polarization in linear regime using DKM formula
- Energy scans using two error seeds generated from the effective model
- Six first order spin-orbit resonances between two integer spin tunes

$(\Delta y)_{\text{rms}} = 43.7\,\mu\text{m}$

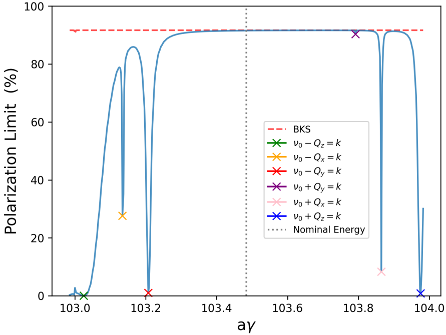

91.6% near nominal energy

$(\Delta y)_{\text{rms}} = 148\,\mu\text{m}$

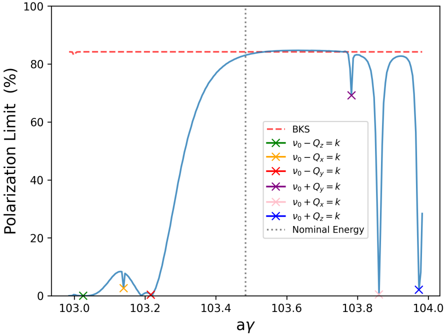

84.6% near nominal energy

Robustness of the Error Generation Method

- The effective model is an efficient way for the proceeding of the current spin polarization research
- 100 error seeds were generated to check the robustness of the effective model

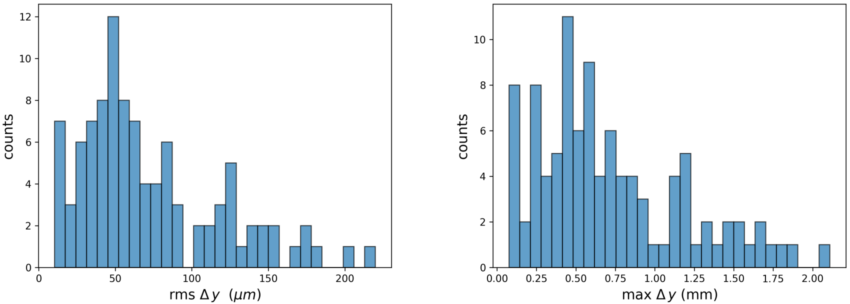

Figure: Distribution of the rms (left) and maximum (right) vertical orbits deviation of 100 produced errors

Robustness of lattice should be checked and guaranteed

Spin Tune Bias

measured spin tune $\neq a\gamma$

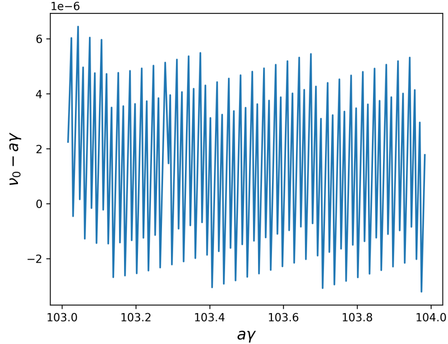

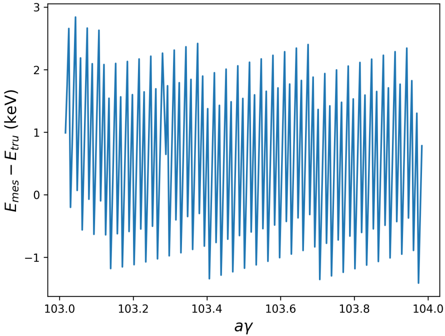

Figure: Spin tune shift from $a\gamma$ (left) and measured energy deviation (right) using the error seed that creates an orbit distortion of $(\Delta y)_{\text{rms}} = 148\,\mu$m

Requirement for center-of-mass energy determination is ± 4 keV at Z energy*

* Alain Blondel, PED Overview: Centre-of-mass energy calibration, FCC Week 2022

Benchmark between Tao (BMAD) and SITF

- SITF, the linear spin simulation module in SITROS
- Both SITF and Tao (BMAD) belong to SLIM family
- Underlying differences between two codes exist $\rightarrow$ check step by step

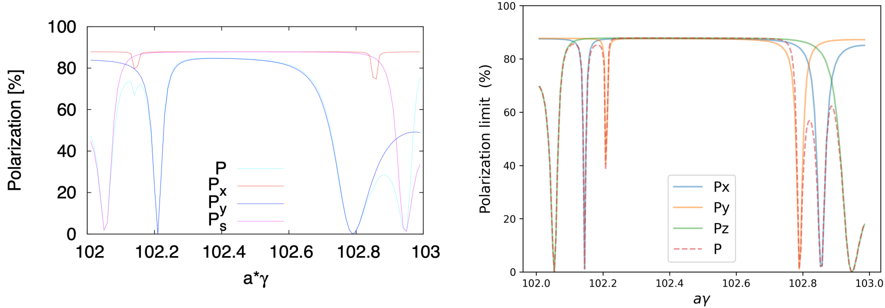

Figure: Energy scan using sequence version 213 seed 13 in SITF (left) and Tao (right)

SITF plot is from Eliana Gianfelice-Wendt

Global Parameter Comparisons

- FCC-ee clean lattice No.217 without misalignments at 45.6 GeV

	Q_x	Q_y	Q_z	x_{rms} [mm]	y_{rms} [mm]	β_x at IP.1 [m]	β_y at IP.1 [mm]
MADX	269.1354	269.2105	0.0247	0.027	0	0.1495	0.8
Tao	269.1354	269.2105	0.0247	0.027	0	0.1495	0.8
SITF	269.1354	269.2108	0.0247	0.027	0	0.1495	0.8

- Simple lattice with 10 nm x and y misalignments in one IR quadrupole (QC1L1.1)

	Q_x	Q_y	Q_z	x_{rms} [mm]	y_{rms} [mm]	β_x at IP.1 [m]	β_y at IP.1 [mm]
MADX	269.1354	269.2105	0.0247	0.027	0.004	0.1495	0.8
Tao	269.1354	269.2105	0.0247	0.027	0.004	0.1495	0.8
SITF	269.1354	269.2106	0.0247	0.027	0.004	0.1495	0.8

Closed Orbit Comparisons

EPFL

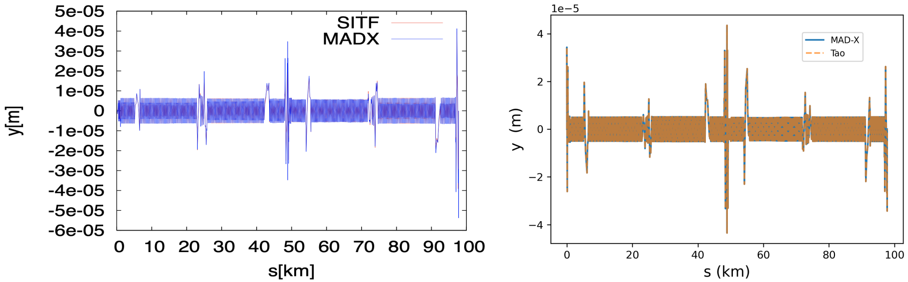

Figure: Vertical closed orbits comparison between MAD-X and SITF (left), and MAD-X and Tao (right)

Tao and SITF create nearly the same closed orbit

SITF plot is from Eliana Gianfelice-Wendt

$\hat{n}_0$ Deviation Comparison

- $\hat{n}_0$, the central quantity for the spin polarization description
- Away from integer spin tune $\Rightarrow$ $\hat{n}_0$ almost aligned with the vertical
- Near integer spin tune $\Rightarrow$ $\hat{n}_0$ deviates from the vertical

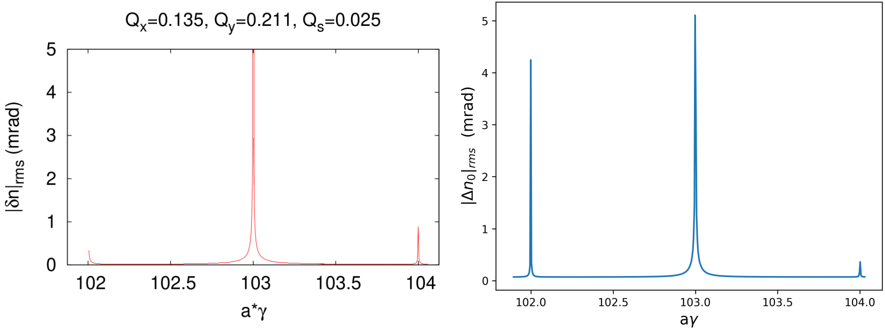

Figure: Variation of the rms $\hat{n}_0$ deviation from the vertical in SITF (left) and Tao (right)

SITF plot is from Eliana Gianfelice-Wendt

Benchmark between Tao, SITF and SLIM

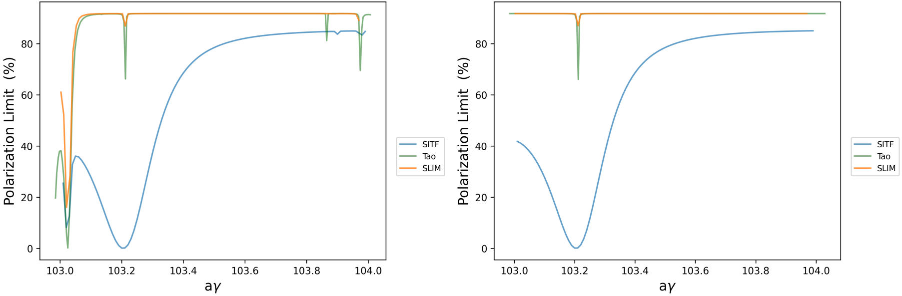

Figure: Energy scan of the equilibrium polarization (left) and the vertical mode polarization (right) by three codes

Tao and SITF share the same BKS level.

The difference may lie in the computation for the spin-orbit coupling function $\partial\hat{n}/\partial\delta$.

SITF and SLIM data are from Eliana Gianfelice-Wendt

Discussions Regarding the Damping in Transport Matrix

EPFL

Thanks to Eliana Gianfelice-Wendt!

- In SLIM/Tao linear calculation undamped 8×8 transport matrix is used for polarization.
- In SITF/SITROS tracking the damped transport matrix is used between emission points.
- Two codes agree when damped matrix is used

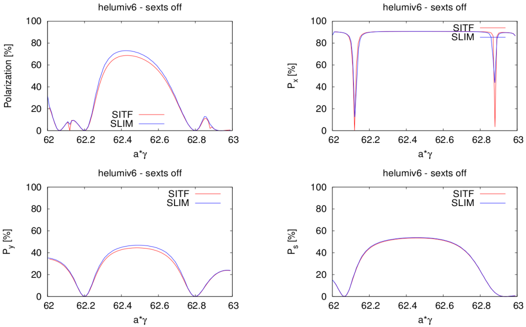

Details will be presented by Eliana Gianfelice-Wendt at EPOL2022

Nonlinear Spin Tracking

- The higher order resonances may become prominent at high energies and affect the achievable polarization level
- Reveal all effects of lattice imperfections on spin polarization
- Long-Term Tracking module in BMAD
- Track the polarization level turn by turn and extract τ_{dep}

$$P_{eq} \simeq P_{BKS} \frac{\tau_{dep}}{\tau_{BKS} + \tau_{dep}}$$

Long-Term Tracking in BMAD

$\nu_0 = m + Q_y - Q_s$

10 electrons

$P_{eq} = 0.15\%$

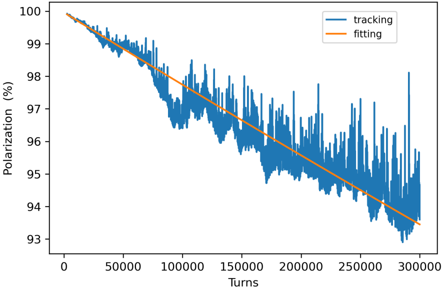

RMSE=0.59
$R^2 = 0.89$

500 electrons

$P_{eq} = 0.099\%$

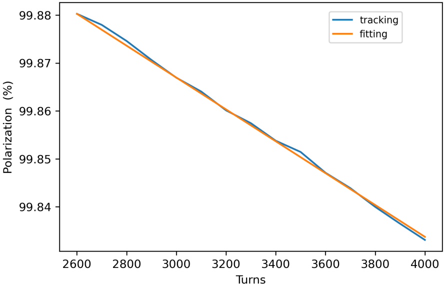

RMSE=4.4×10^{-4}
$R^2 = 0.999$

Using more particles improves the fitting precision but needs more time.

Root-mean-square error, RMSE = $\sqrt{\sum_{i=1}^{N}(P - P*)^2/N}$

Preliminary Results of Nonlinear Spin Tracking

1000 particles, 7000 turns, PTC

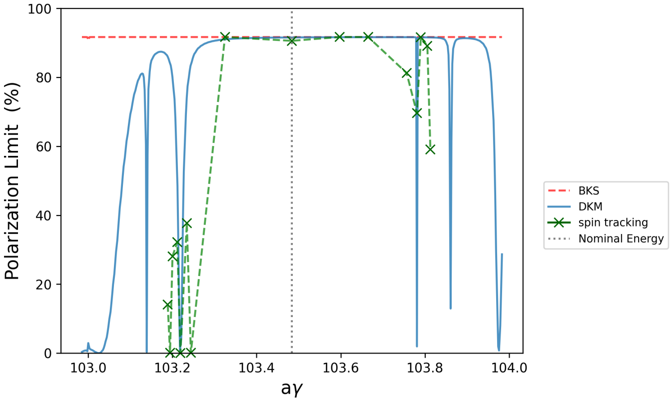

Main Problems Now

- Achievable polarization level is based on orbits $\Rightarrow$ robust lattice
- How can a high transverse polarization level be guaranteed?
- How precise can the beam energy be measured using resonant depolarization?

What are we working on?

- Resonant depolarization simulation (with David Sagan)
- Lattice corrections of FCC-ee in MADX (with optics group)
- Orbit bumps for transverse polarization optimization
- Optics corrections and spin simulations in LEP (with Werner Herr)
- Harmonic corrections (with Desmond Barber and Werner Herr)

Thank you!

Match the main parameters with the designed value

EPFL

- Simplified matching: using the elements in RF section
- Optimized matching: adding BPMs, kickers and correctors

Attributes	Designed value	With RF Section	With Kickers, Correctors	Deviation (%)
β_x^* at IP.1/4 (m)	0.15	0.15	0.15	0
β_y^* at IP.1/4 (mm)	0.8	0.7977	0.79941	0.074
β_x^* at IP.2/3 (m)	0.15	0.15	0.15	0
β_y^* at IP.2/3 (mm)	0.8	0.79	0.79947	0.066
x at IP.1/4 (nm)	0	-180	10	N.A.
z at IP.1/4 (nm)	0	20	1.5	N.A.
x at IP.2/3 (nm)	0	-270	390	N.A.
z at IP.2/3 (nm)	0	-20	1.5	N.A.
Synchrotron tune Q_s	0.025	0.0247	0.025	0
Horizontal tune Q_x	269.139	269.139	269.139	0
Vertical tune Q_y	269.219	269.219003	269.219	0

Spin-Orbit Coupling Function Comparison

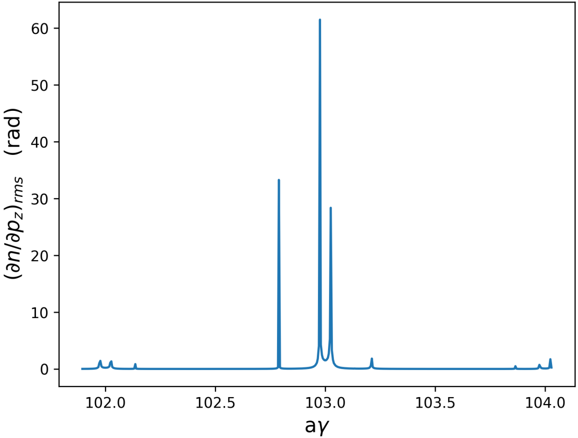

Figure: Variation of the rms spin-orbit coupling function $\partial \hat{n}/\partial \delta$ computed by Tao

Energy Scan Comparison with Simple Lattice

- Main difference comes from the vertical mode polarization

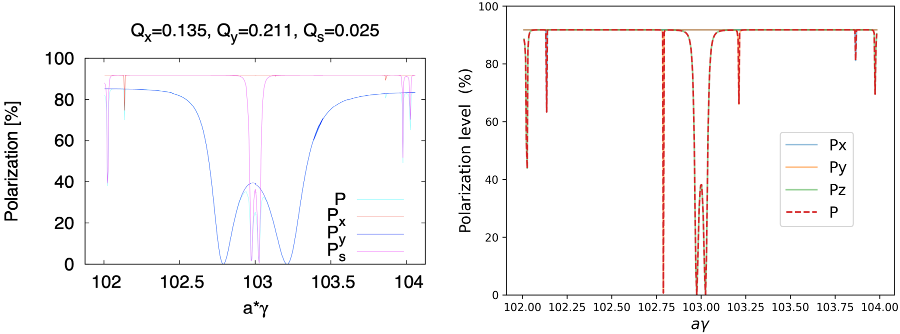

Figure: Energy scans using the simple lattice with one misalignment in SITF (left) and Tao (right)

SITF plot is from Eliana Gianfelice-Wendt

Spin Precession

The spin precession under electromagnetic field can be described by the Thomas-BMT equation

$$\frac{\mathrm{d}\hat{S}}{\mathrm{d}s} = \left(\vec{\Omega}^{c.o}(s) + \vec{\omega}^{s.b}(\vec{u}; s)\right) \times \hat{S}$$

$$\vec{\Omega}^{c.o}(s + C) = \vec{\Omega}^{c.o}(s)$$

$$\vec{u} \equiv (x, x', y, y', z, \delta)$$

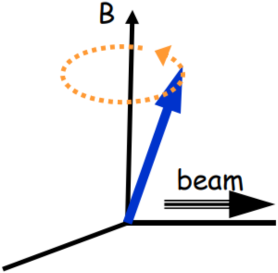

Figure from Bai, M. (2010, December). Polarized protons and siberian snakes.

Closed Orbit Solution

Spin rotation matrix can be used to express the transformation

$$\hat{S}(s) = \mathbf{R}_{c.o}(s, s_i)\hat{S}(s_i)$$

$\hat{n}_0(s)$

- the unit length eigenvector that corresponds to the unit eigenvalue
- the periodic and stable spin direction on the closed orbit
- the precession axis for spins on the closed orbit
- spin basis $(\hat{n}_0(s), \hat{m}_0(s), \hat{l}_0(s))$ for the spin motion description

ν_0

- closed orbit spin tune
- the number of spin processions around $\hat{n}_0$ per turn on the closed orbit
- $\nu_0 = a\gamma$ in the perfectly aligned flat ring without solenoids
- $\nu_0 \neq a\gamma$ in general

Summary

- The first-stage exploration of the FCC-ee spin simulations using BMAD shows promising results
- Linear polarization simulations offer a proof of concept, manifesting the influence of the 1st order resonances
- Benchmarks with SITROS in the linear spin calculation regime reveal the influence of damping in the transport matrix used for polarization
- First attempts at nonlinear spin trackings highlight the technical challenges associated with such simulations
- Detailed discussions are expected in the following EPOL2022 workshop